Supporting Information on

Efficient photoreduction of hexavalent uranium over defective ZnO nanoparticals by oxygen defect engineering

Xiaochuan Deng[a,1], Geng Zou[a,1], Boyuan Tu[a,c,1], Mingfang Hu[b], Wenkun Zhu[a,*], Rong He[a,*] , Tao Chen[a,*]

[a]State Key Laboratory of Environment-friendly Energy Materials, National Co-innovation Center for Nuclear Waste Disposal and Environmental Safety, Sichuan Co-Innovation Center for New Energetic Materials, Nuclear Waste and Environmental Safety Key Laboratory of Defense, School of National Defence Science & Technology, Southwest University of Science and Technology, Mianyang 621010, China.

[b]School of Life Science and Engineering, Southwest University of Science and Technology, Sichuan Mianyang 621010, China.

[c]School of Mathematics and Physics, Southwest University of Science and Technology, Sichuan Mianyang 621010, China.

1 These authors contributed equally.

* Corresponding authors.

E-mail addresses: zhuwenkun@swust.edu.cn (W. Zhu), her@swust.edu.cn (R. He) , and chent@swust.edu.cn (T. Chen).

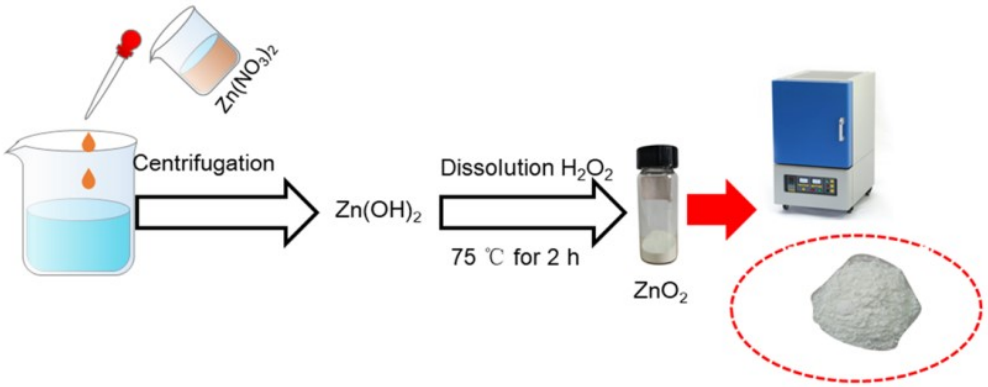

Figure S1. Schematic illustration for the preparation procedure of ZnO with oxygen vacancies.

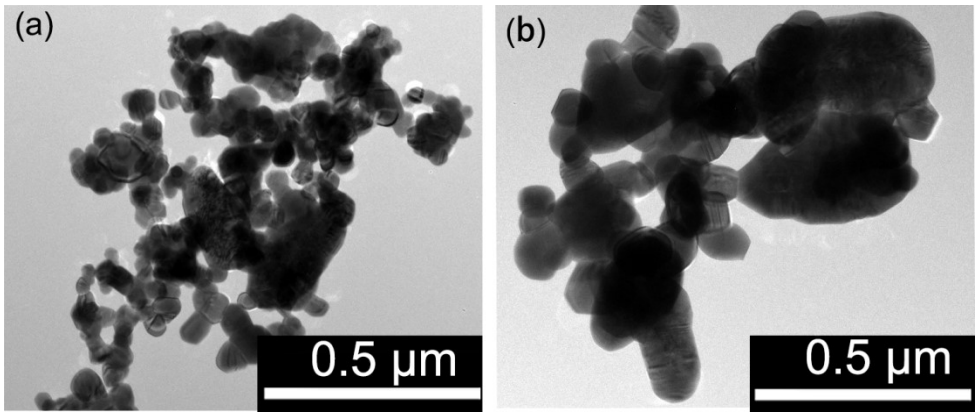

Figure S2 (a) TEM image of ZnO-600; (b) TEM image of ZnO-800.

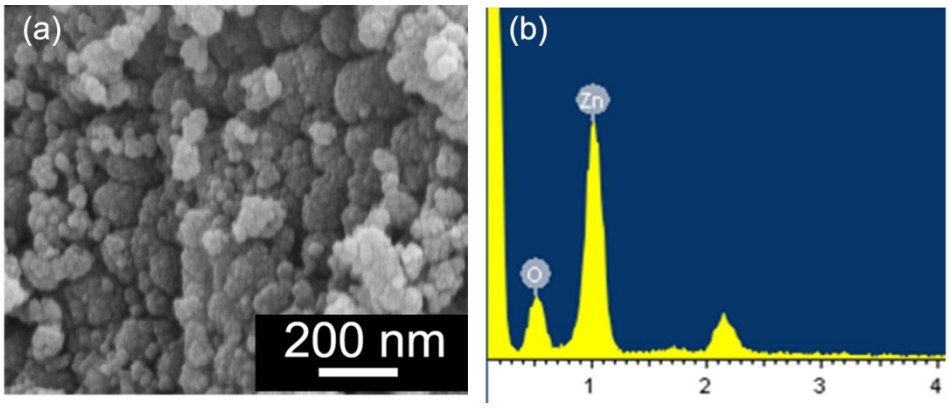

Figure S3 (a) SEM pattern of ZnO-400 and corresponding EDS(b).

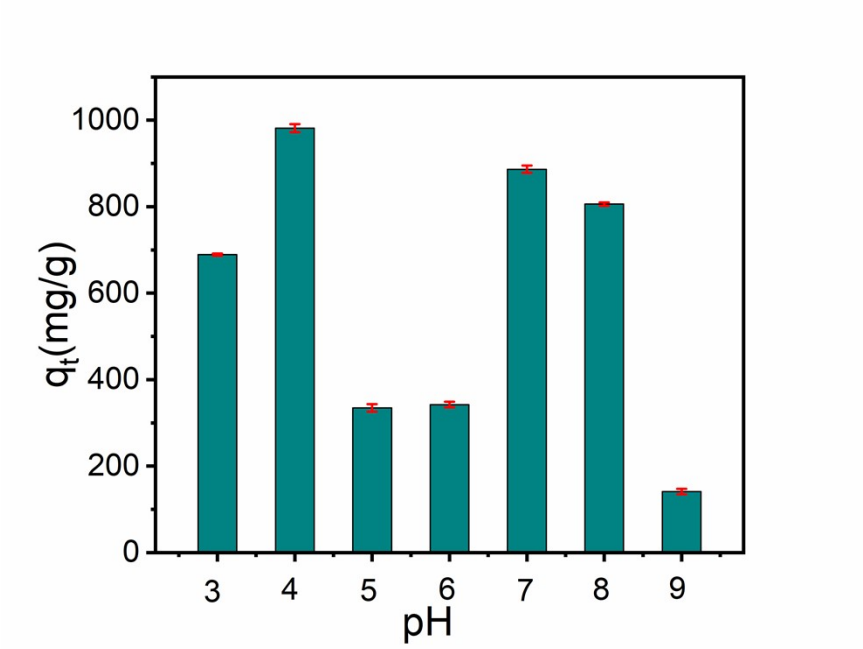

Figure S4. The ability to remove U(VI) at different pH values.

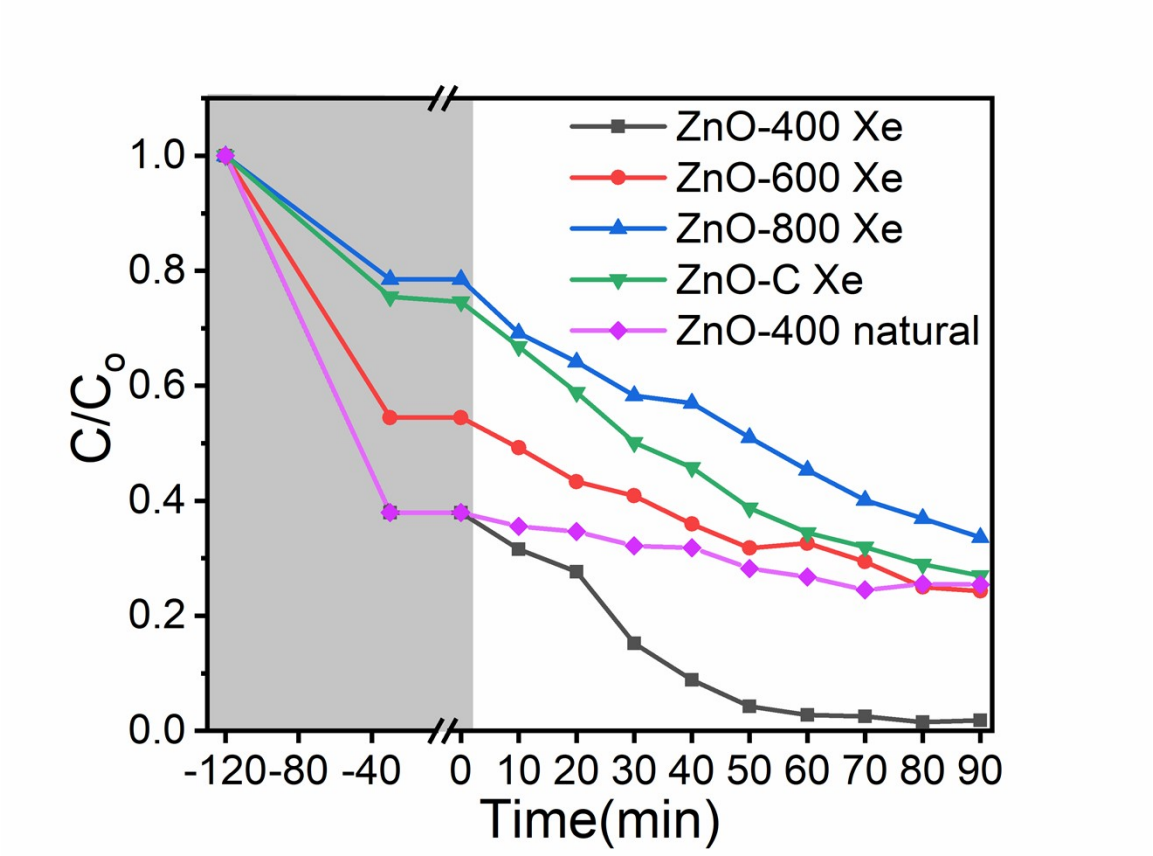

Figure S5. At pH =4, the variation of UO_2^{2+} concentration vs. contact time with ZnO-400, ZnO-600, ZnO-800 , ZnO-C under Xe lamp and ZnO-400 under natural light.

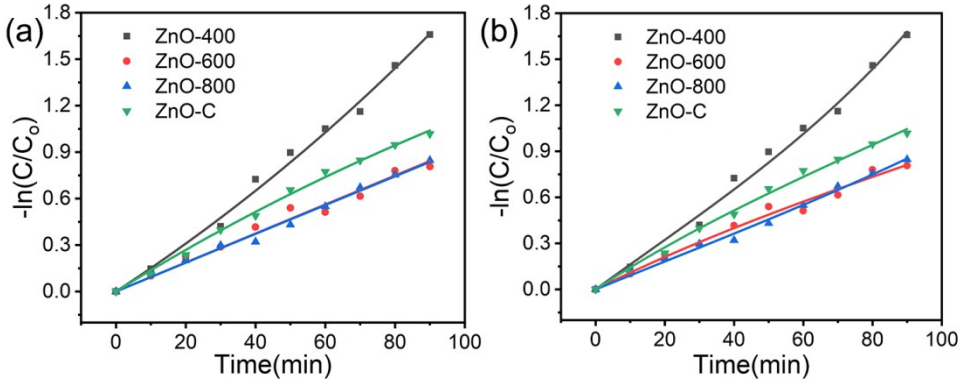

Figure S6. (a)Pseudo-frist-order model and Pseudo-secend-order model(b).

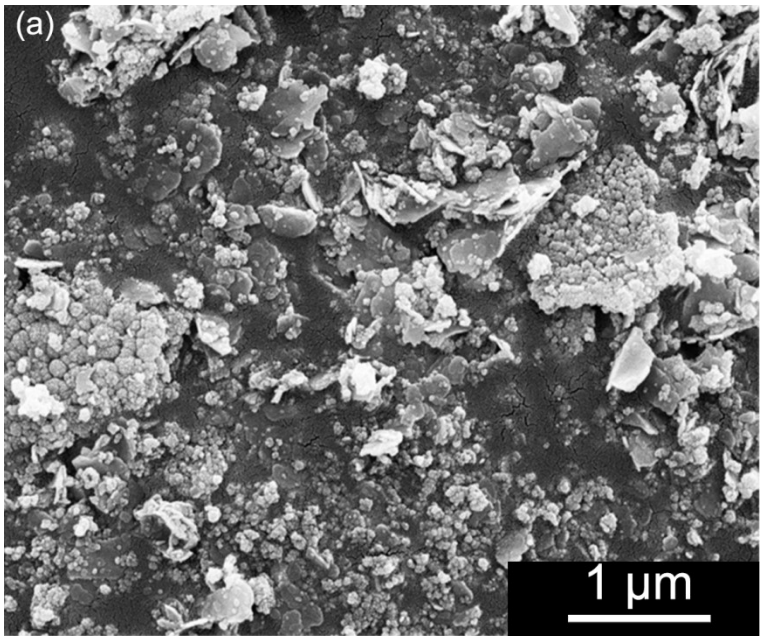

Figure S7. SEM image of Used ZnO-400.

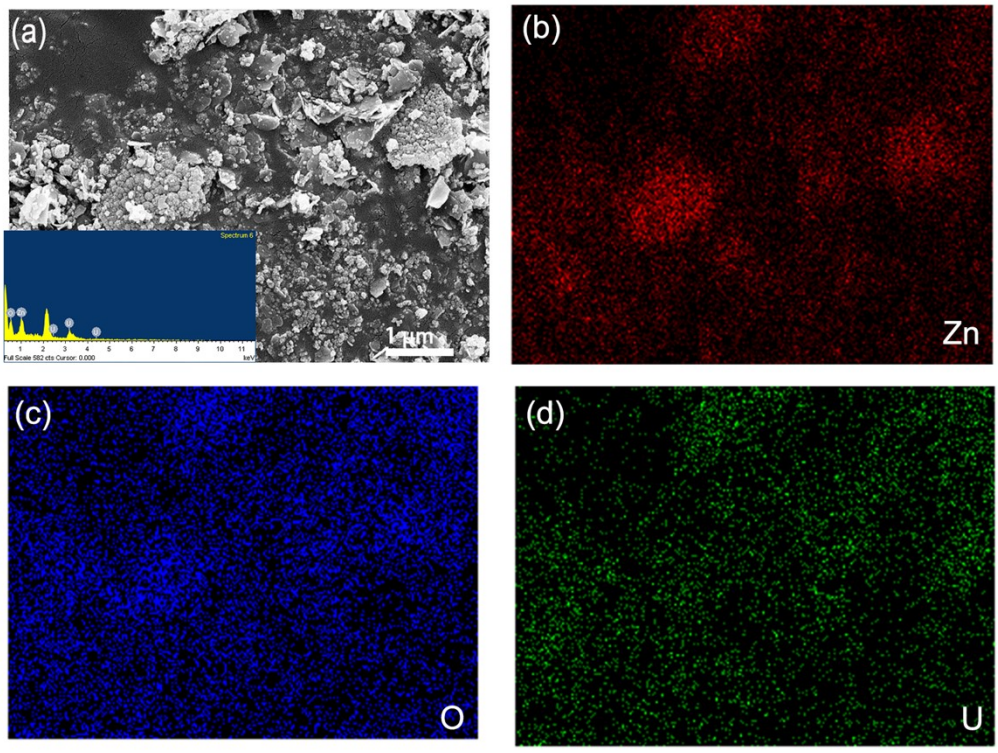

Figure S8. (a) Used ZnO-400 SEM and EDS; (b) the corresponding area EDS-mapping of Zn, (c) O, (d) U.

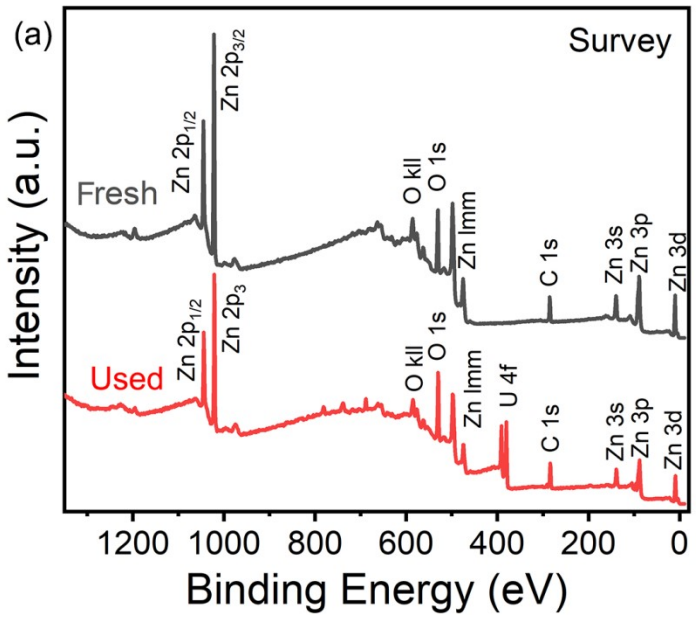

Figure S9. XPS spectra of Fresh ZnO-400 and Used ZnO-400.

Table S1. The maximum U (VI) removal ability on different photocatalysts.

Photocatalysts	Experimental conditions	Photocatalytic equilibrium time (min)	Removal rate (%)	Reference
g-C_3N_4/TiO_2	C_0=20 mg/g, T=293 K	180	83	1
Nb/TiNFs	C_0=20 mg/L, pH=5.0, T=303K	240	89.3%	2
TiO_2	C_0=125.5 mg/L, pH=3, T=298K	30	90	3
MOF PCN-222	C_0= 1-400 mg/g, pH=4, T=300 K	20-1200	96.7	4
SCU-19	C_0=10 mg/L, pH=4, T=303K	1500	99	5
TiO_2	C_0= 0.1 mM, pH=6.0, T=293 K	200	62	6
$SrTiO_3$/TiO_2	C_0=100 mg/L, pH=4.0, T=293K	210	80	7
B-g-C_3N_4	C_0=60 mg/L, pH=7.0, T=293K	20	93	8
TiO_2	C_0= 0.1 mM, pH=5.0, T=313 K	200	~96	9
mesoporous g-C_3N_4	C_0= 0.5 mM, pH=6.0, T=293K	140	~95	10
mGO/g-C_3N_4	C_0= 20 mg/g, pH=6.0, T=298 K	1440	96.2	11
TiO_2/RGO/Fe_3O_4	C_0= 0.4 mM, pH=4.0, T=293 K	180	~92	12
Fe_2O_3-graphene oxide	C_0=5 mg/L, pH=4.0, T=293K	180	75	13
PC_3N_4	C_0= 0.12 mM, pH=7.0, T=298 K	20	90	14
BC-MoS_{2-x}	C_0= 8 mg/g, pH=5.5, T=298 K	40	92	15
MoS_x/RGO	C_0= 8 mg/g, pH=5.5, T=298 K	30	91.6	16

LMCT	C_0= 50 mg/g, pH=5.5, T=298 K	120	95	17
TTT–DTDA	C_0= 10 mg/g, pH=5, T=300 K	600	94.7	18
Carboxylated g-C_3N_4	C_0= 0.1 mM, pH=8.2, T=298 K	50	100	19
CdS/g-C_3N_4	C_0= 0.1 mM, pH=6.0, T=298 K	50	100	20
3D RGO@TiO_2-3	C_0= 50 mg/g, pH=6.0, T=298 K.	140	99.5	21
3D GA/TiO_2	C_0= 20 mg/g, pH=6.0, T=298 K.	40	60	22
MnO_x/UiO-66/$Ti_3C_2T_x$	C_0= 20 mg/g, pH=6.0, T=298 K.	60	98.4	23
C_3N_5/RGO	C_0= 10 mg/g, pH=5, T=300 K.	100	94.9	24
C_3N_5/GO	C_0= 10 mg/g, pH=6, T=300 K.	60	96.1	25
ZnO-400	C_0=200 mg/L, pH=4.0, T=298 K.	210	98.5	This work

Reference

1. Jiang, X.; Xing, Q.; Luo, X.; Li, F.; Zou, J.; Liu, S.; Li, X.; Wang, X., Simultaneous photoreduction of Uranium(VI) and photooxidation of Arsenic(III) in aqueous solution over g-C_3N_4/TiO_2 heterostructured catalysts under simulated sunlight irradiation. *Applied Catalysis B-environmental* 2018, 228, 29-38.

2. Liu, X.; Du, P.; Pan, W.; Dang, C.; Qian, T.; Liu, H.; Liu, W.; Zhao, D., Immobilization of uranium(VI) by niobate/titanate nanoflakes heterojunction through combined adsorption and solar-light-driven photocatalytic reduction. *Applied Catalysis B-environmental* 2018, 231, 11-22.

3. Salomone, V. N.; Meichtry, J. M.; Litter, M. I., Heterogeneous photocatalytic removal of U(VI) in the presence of formic acid: U(III) formation. *Chemical Engineering Journal* 2015, 270, 28-35.

4. Li, H.; Zhai, F.; Gui, D.; Wang, X.; Wu, C.; Zhang, D.; Dai, X.; Deng, H.; Su, X.; Diwu, J., Powerful uranium extraction strategy with combined ligand complexation and photocatalytic reduction by postsynthetically modified photoactive metal-organic frameworks. *Applied Catalysis B-environmental* 2019, 254, 47-54.

5. Zhang, H.; Liu, W.; Li, A.; Zhang, D.; Li, X.; Zhai, F.; Chen, L.; Chen, L.; Wang, Y.; Wang, S., Three Mechanisms in One Material: Uranium Capture by a Polyoxometalate-Organic Framework through Combined Complexation, Chemical

Reduction, and Photocatalytic Reduction. *Angewandte Chemie* 2019, 58, 16110-16114.
6. Li, P.; Wang, J.; Peng, T.; Wang, Y.; Liang, J.; Pan, D.; Fan, Q., Heterostructure of anatase-rutile aggregates boosting the photoreduction of U(VI). *Applied Surface Science* 2019, 483, 670-676.
7. Hu, L.; Yan, X.; Zhang, X.; Shan, D., Integration of adsorption and reduction for uranium uptake based on $SrTiO_3/TiO_2$ electrospun nanofibers. *Applied Surface Science* 2018, 428, 819-824.
8. Lu, C.; Chen, R.; Wu, X.; Fan, M.; Liu, Y.; Le, Z.; Jiang, S.; Song, S., Boron doped g-C3N4 with enhanced photocatalytic UO_2^{2+} reduction performance. *Applied Surface Science* 2016, 360, 1016-1022.
9. Li, P.; Wang, J.; Wang, Y.; Liang, J.; He, B.; Pan, D.; Fan, Q.; Wang, X., Photoconversion of U(VI) by TiO_2: An efficient strategy for seawater uranium extraction. *Chemical Engineering Journal* 2019, 365, 231-241.
10. Wang, J.; Wang, Y.; Wang, W.; Ding, Z.; Geng, R.; Li, P.; Pan, D.; Liang, J.; Qin, H.; Fan, Q., Tunable mesoporous g-C_3N_4 nanosheets as a metal-free catalyst for enhanced visible-light-driven photocatalytic reduction of U(VI). *Chemical Engineering Journal* 2020, 383, 123193.
11. Dai, Z.; Sun, Y.; Zhang, H.; Ding, D.; Li, L., Photocatalytic reduction of U(VI) in wastewater by mGO/g-C_3N_4 nanocomposite under visible LED light irradiation. *Chemosphere* 2020, 254, 126671.
12. Li, Z.; Huang, Z.; Guo, W.; Wang, L.; Zheng, L.; Chai, Z.; Shi, W., Enhanced Photocatalytic Removal of Uranium(VI) from Aqueous Solution by Magnetic TiO_2/Fe_3O_4 and Its Graphene Composite. *Environmental Science & Technology* 2017, 51, 5666-5674.
13. Guo, Y.; Guo, Y.; Wang, X.; Li, P.; Kong, L.; Wang, G.; Li, X.; Liu, Y., Enhanced photocatalytic reduction activity of uranium(VI) from aqueous solution using the Fe_2O_3–graphene oxide nanocomposite. *Dalton Transactions* 2017, 46, 14762-14770.
14. Wu, X.; Jiang, S.; Song, S.; Sun, C., Constructing effective photocatalytic purification system with P-introduced g-C_3N_4 for elimination of UO_2^{2+}. *Applied Surface Science* 2018, 430, 371-379.
15. Chen, T.; Liu, B.; Li, M.; Zhou, L.; Lin, D.; Ding, X.; Lian, J.; Li, J.; He, R.; Duan, T.; Zhu, W., Efficient uranium reduction of bacterial cellulose-MoS_2 heterojunction via the synergistically effect of Schottky junction and S-vacancies engineering. *Chemical Engineering Journal* 2021, 406, 126791.
16. Chen, T.; Li, M.; Zhou, L.; Feng, X.; Lin, D.; Ding, X.; Li, C.; Yan, R.; Duan, T.; He, R.; Zhu, W., Harmonizing the energy band between adsorbent and semiconductor enables efficient uranium extraction. *Chemical Engineering Journal* 2021, 420, 127645.
17. Li, S.; Hu, Y.; Shen, Z.; Cai, Y.; Ji, Z.; Tan, X.; Liu, Z.; Zhao, G.; Hu, S.; Wang, X., Rapid and selective uranium extraction from aqueous solution under visible light in the absence of solid photocatalyst. *Science China Chemistry* 2021, 64, 1323-1331.
18. Song, Y.; Li, A.; Li, P.; He, L.; Xu, D.; Wu, F.; Zhai, F.; Wu, Y.; Hu, K.; Wang, S.; Sheridan, M. V., Unassisted Uranyl Photoreduction and Separation in a Donor–Acceptor

Covalent Organic Framework. *Chemistry of Materials* 2022, 34, 2771-2778.
19. Li, P.; Wang, Y.; Wang, J.; Dong, L.; Zhang, W.; Lu, Z.; Liang, J.; Pan, D.; Fan, Q., Carboxyl groups on g-C_3N_4 for boosting the photocatalytic U(VI) reduction in the presence of carbonates. *Chemical Engineering Journal* 2021, 414, 128810.
20. Li, P.; Wang, J.; Wang, Y.; Dong, L.; Wang, W.; Geng, R.; Ding, Z.; Luo, D.; Pan, D.; Liang, J.; Fan, Q., Ultrafast recovery of aqueous uranium: Photocatalytic U(VI) reduction over CdS/g-C_3N_4. *Chemical Engineering Journal* 2021, 425, 131552.
21. Dong, Z.; Zhang, Z.; Li, Z.; Feng, Y.; Dong, W.; Wang, T.; Cheng, Z.; Wang, Y.; Dai, Y.; Cao, X.; Liu, Y.; Liu, Y., 3D structure aerogels constructed by reduced graphene oxide and hollow TiO_2 spheres for efficient visible-light-driven photoreduction of U(vi) in air-equilibrated wastewater. *Environmental Science: Nano* 2021, 8, 2372-2385.
22. Yu, S.; Wei, D.; Shi, L.; Ai, Y.; Zhang, P.; Wang, X., Three-dimensional graphene/titanium dioxide composite for enhanced U(VI) capture: Insights from batch experiments, XPS spectroscopy and DFT calculation. *Environmental Pollution* 2019, 251, 975-983.
23. Yu, K.; Tang, L.; Cao, X.; Guo, Z.; Zhang, Y.; Li, N.; Dong, C.; Gong, X.; Chen, T.; He, R.; Zhu, W., Semiconducting Metal–Organic Frameworks Decorated with Spatially Separated Dual Cocatalysts for Efficient Uranium(VI) Photoreduction. *Advanced Functional Materials* 2022, 32, 2200315.
24. Wu, L.; Yang, X.; Chen, T.; Li, Y.; Meng, Q.; Zhu, L.; Zhu, W.; He, R.; Duan, T., Three-dimensional C_3N_5/RGO aerogels with enhanced visible-light response and electron-hole separation efficiency for photocatalytic uranium reduction. *Chemical Engineering Journal* 2022, 427, 131773.
25. Meng, Q.; Yang, X.; Wu, L.; Chen, T.; Li, Y.; He, R.; Zhu, W.; Zhu, L.; Duan, T., Metal-free 2D/2D C_3N_5/GO nanosheets with customized energy-level structure for radioactive nuclear wastewater treatment. *Journal of Hazardous Materials* 2022, 422, 126912.